



Instability of condensate film and capillary blocking in small-diameter-thermosyphon condensers

H. Teng, P. Cheng*, T.S. Zhao

Department of Mechanical Engineering, The Hong Kong University of Science and Technology, Clear Water Bay, Kowloon, Hong Kong

Received 23 April 1998; received in revised form 2 December 1998

Abstract

Instability of the condensate film in a small-diameter-tube condenser was investigated by using an integro-differential approach. The disturbance wave parameters were predicted based on the characteristic equation derived in this study, and the results were in good agreement with the available experimental data reported in the literature. Capillary blocking taking place in a small-diameter-thermosyphon condenser was also examined. The proposed mechanism for capillary blocking reasonably explains the observed two-phase-flow phenomena during formation of capillary blocking. © 1999 Elsevier Science Ltd. All rights reserved.

1. Introduction

Convective condensation in tubes is encountered in many applications, such as air-conditioning, refrigeration, and heat-pipe condensers, etc. The concurrent two-phase-flow patterns that typically occur during the condensation process in air-conditioning and refrigeration condensers are annular flow, slug flow, plug flow, and bubbly flow [1]. At low to moderate condensation pressures, the annular flow dominates the condensation process and only a small portion of the flow is of other two-phase patterns. Thus, the condensation heat transfer is primarily associated with the annular flow. While in condensers of gravity-assisted heat pipes, i.e., thermosyphons (where the two-phase flow in opposite directions), the annular flow is the usual two-phase-flow pattern. Owing to either the hydrodynamic force or surface tension, the inner surface of the annular condensate film is inherently unstable and sur-

face waves will form at the vapor–liquid interface [2], resulting in a complicated, unstable flow pattern in the condensate film. In a large-diameter tube where the capillary force is small, the unstable surface waves are caused by the hydrodynamic force, i.e., Kelvin–Helmholtz instability. If the condensate film is thick, then the unstable waves may induce liquid bridging [3–5]. On the other hand, in a small-diameter tube where the capillary force becomes significant, the unstable surface waves are due primarily to Rayleigh instability except for cases with a large phase-velocity difference. Two distinctive capillary flows may be encountered in small-diameter-tube condensers (shown in Fig. 1): if the condensate film is thin, the surface deformation of the condensate film may lead to a capillary-collar flow; if the condensate film is thick, the instability of the condensate film may cause liquid bridging, which cuts the vapor core into bubbles, resulting in a capillary-bubble flow [1,6,7].

These aforementioned liquid bridgings may be encountered in both concurrent and countercurrent condensers. In large-diameter (either concurrent or

* Corresponding author..

Nomenclature

a	undisturbed radius of inner surface of condensate film
A	cross-sectional area of condensate film
A_{collar}	vapor–liquid interface area of condensate collar
C	mean curvature of condensate collar
g	gravitational acceleration
k	disturbance wavenumber ($\equiv 2\pi/\lambda$)
l_{bridge}	width of liquid bridge
L	latent heat
m	film-thickness parameter ($\equiv r_0^2/a^2 - 1$)
n	film-thickness parameter [$\equiv 1 - 3R^2 + (4R^4 \ln R)/m$]
n_j	projection of unit outward normal in j th-direction
p	pressure
r_0	tube radius
r_B	mean radius of the bottom vapor–liquid interface of liquid bridge
r_s	disturbed radius of inner surface of condensate film
r_T	mean radius of the top vapor–liquid interface of liquid bridge
R	film-thickness parameter ($\equiv r_0/a$)
S	surface area of the condensate film
t	time
t_b	wave-breakup time
T	temperature
u_i	velocity component in i th-direction
\hat{u}	component of vapor-velocity vector induced by surface disturbance
\hat{u}^v	velocity vector for vapor
U	prescribed vapor core velocity
V	volume of condensate film
V_{collar}	volume of condensate collar
\tilde{W}_e	Weber number ($\equiv 2a\hat{\rho}U^2/\sigma$)
Z	modified Ohnesorge number [$\equiv (3 + R^2)\mu/(2a\rho\sigma)^{1/2}$]

Greek symbols

α	disturbance amplitude
α_0	initial disturbance amplitude
β	dimensionless growth rate in amplitude [$\equiv \omega(2\rho a^3/\sigma)^{1/2}$]
δ	thickness of condensate film
ϵ_{ij}	strain-rate tensor
η	dimensionless wavenumber ($\equiv ka$)
κ	thermal conductivity
λ	disturbance wavelength
μ	viscosity
ρ	density
σ	surface tension
τ_{ij}	stress tensor
ϕ	velocity potential
ω	dimensional growth rate in amplitude

Subscripts

cr	critical property of condensate collar
m	property of most-unstable wave
s	property at interface

Index

()	property of vapor phase
-----	-------------------------

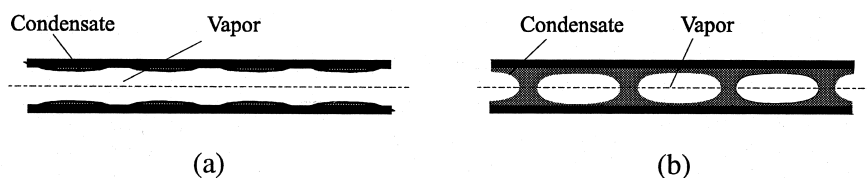


Fig. 1. Selected two-phase-flow patterns in small-diameter-tube condensers: (a) capillary-collar flow; (b) capillary-bubble flow.

countercurrent flow) condensers and small-diameter concurrent-flow condensers, liquid bridges usually do not block the flow because either liquid bridges are unstable and break up due to the hydrodynamic force (in countercurrent flows) or bubbles between liquid bridges are converted rapidly into liquid due to condensation heat transfer (in concurrent flows). However, in the condenser of a small-diameter thermosyphon, i.e., a countercurrent flow condenser with a dead end, liquid bridges resulting from the condensate-film instability may severely affect working conditions of the thermosyphon if the driving force for the condensate flow is not large enough to overcome the flow resistance. As a result, a liquid plug may form and block the dead end of the condenser (this phenomenon is known as capillary blocking), which, in turn, may result in partial dryout in the evaporator because the blocked working fluid cannot return to the evaporator.

Capillary blocking in condensers of small-diameter thermosyphons has been reported by [8,9]. Vasil'ev et al. pointed out that capillary blocking may occur commonly in thermosyphon condensers if the tube diameter is small and the condensate film is thick. A theoretical investigation of capillary blocking in a small-diameter-thermosyphon condenser was reported previously by [8]. Their analysis was based on the assumptions that no surface waves are formed at the vapor–liquid interface and that capillary blocking is due to the condensate film merger. However, these assumptions may be challenged on the basis of experimental observations [6,9–12] that the inner surface of the annular liquid film in a tube is always unstable which induces surface waves at the inner surface of the film, and that instability of the surface waves often result in multiple liquid bridges which cannot be explained by the mechanism of the condensate film merger. In addition, with an appropriate charging rate of the working fluid, film merger may not occur anywhere in a thermosyphon. Therefore, capillary blocking most probably is caused by liquid bridging. To date, little work on instability of the condensate film in small-diameter-tube condensers has been reported in the literature.

Recently, micro heat pipes (both with wick and wickless) show considerable promise for the cooling of electronic equipment [13,14]. Although the majority of the wickless micro heat pipes have a polygonal cross

section, cylindrical vapor–liquid interface and some phenomena that occur in a small-diameter-thermosyphon (such as the formation of a liquid plug at the dead end of the condenser and partial dryout in the evaporator) are also encountered in these micro heat pipes [13,14]. Therefore hydrodynamic behavior of the condensate in a small-diameter-thermosyphon may also reflect some characteristics of that in wickless micro heat pipes. The objectives of this study are: (1) to analyze instability of the annular condensate film in a tube which is encountered in both concurrent flow and countercurrent condensers, and (2) to examine the mechanism for capillary blocking which occurs in small-diameter-thermosyphon condensers.

There are essentially two theoretical approaches that can be used to study the capillary instability: the first one is the integro-differential approach by Rayleigh [2,15], and the second one is the conventional approach of solving the complete set of the differential equations [10]. In the present work, we will adopt Rayleigh's approach because it will lead to a characteristic equation that is explicit and the real form. This characteristic equation, in the limiting cases of low vapor velocities and high vapor velocities, will be examined. Applications to capillary blocking in a small-diameter-thermosyphon condenser will be illustrated.

2. Instability of the condensate film in a tube

In this section, we will analyze instability of the condensate film in a tube and derive a characteristic equation describing stability or instability of the disturbance waves that may form on the condensate film.

2.1. Governing equations

The flow system under study is an axisymmetric, viscous annular condensate film on the inner surface of a cylindrical tube of radius r_0 , and a vapor core in the center of the tube (shown in Fig. 2). Since the disturbed flow of the condensate is of interest, for simplicity, both the liquid and vapor phases are assumed to move at their phase velocities. Since only the difference in phase velocities influences instability of the condensate film, a cylindrical polar system is chosen that

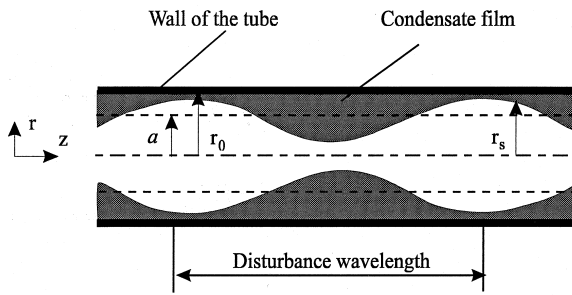


Fig. 2. Flow system configuration.

translates with the phase velocity of the condensate film (note that the phase velocity of the condensate film is very low in a small-diameter tube); thus, any other motions in the condensate film may be assumed to be insignificant in comparison to that induced by surface disturbances. Because the phenomenon under consideration is periodic along the length of the tube, only a single wavelength will be considered. Because that changes in thickness of the condensate film and the vapor velocity are very small over one wavelength, we may assume that the thickness of the condensate film is constant and that the vapor core has an undisturbed radius a and a prescribed uniform (relative) velocity U . It is further assumed that heat and mass transfer affect the film instability only indirectly via the film thickness and that both the condensate and the vapor are Newtonian fluids and incompressible. In addition, we may assume that the influence of the gravitational force on the film instability may be neglected in comparison to that of interfacial forces for small-diameter tubes.

Following an approach employed by Rayleigh [2,15] to study the instability of cylindrical fluid surfaces, we examine the condensate-film instability via an energy balance on the film on the inner surface of the tube [16,17]:

$$\int_V \frac{\partial}{\partial t} \left(\frac{1}{2} \rho u_i u_i \right) dV = \int_S \tau_{ij} u_i n_j dS - \int_V \tau_{ij} \epsilon_{ij} dV \quad (1)$$

where V and S represent the volume and surface area of the film, t the time, ρ the density of the condensate, u_i the velocity component in the i th-direction, τ_{ij} the stress tensor, n_j the projection of the unit outward normal in the j th-direction, and ϵ_{ij} the strain-rate tensor. In Eq. (1), the left-hand-side represents the rate of increase in kinetic energy of the film while on the right-hand-side, the first term is the rate at which work is performed on the film, and the second term is the rate of energy dissipation in the film. The surface integral in Eq. (1) requires that the interfacial condition and motion of the vapor core be known. Since no

work is performed at the outer surface of the annular condensate film, only work done at the vapor–liquid interface will be considered. The velocity and stress-tensor components in the surface integral in Eq. (1) must satisfy the following interfacial conditions [18] along the vapor–liquid interface:

kinematic conditions

$$u_{rs} = \hat{u}_{rs}, \quad u_{zs} = \hat{u}_{zs} \quad (2)$$

dynamic conditions

$$\tau_{rrs} - \hat{\tau}_{rrs} = \sigma [1/r_s + (\partial^2 r_s / \partial z^2) / (1 + (\partial r_s / \partial z)^2)^{3/2} - 1/a] \quad (3)$$

and

$$\tau_{rzs} - \hat{\tau}_{rzs} \approx 0 \quad (4)$$

where the caret signifies properties of the vapor phase, the subscript s denotes properties at the interface, r_s is the disturbed radius of the inner surface of the film, and σ is the surface tension. The motion of the vapor core may be described by the momentum and the continuity equations:

$$\frac{\partial \hat{\mathbf{u}}^v}{\partial t} + \hat{\mathbf{u}}^v \cdot \nabla \hat{\mathbf{u}}^v = -\frac{1}{\hat{\rho}} \nabla \hat{p} + \frac{\hat{\mu}}{\hat{\rho}} \nabla^2 \hat{\mathbf{u}}^v \quad (5)$$

$$\nabla \cdot \hat{\mathbf{u}}^v = 0 \quad (6)$$

where $\hat{\mathbf{u}}^v = U \mathbf{n}_z + \hat{\mathbf{u}}$ is the vapor velocity, with \mathbf{n}_z being the unit vector in the z -direction and $\hat{\mathbf{u}}$ being the velocity vector induced by the disturbance wave; \hat{p} and $\hat{\mu}$ are, respectively, the pressure and viscosity of the vapor phase.

The stress-tensor components for the vapor core given in Eqs. (3) and (4) can be written as $\hat{\tau}_{rrs} = -\hat{p} + 2\hat{\mu}(\partial \hat{u}_r / \partial r)_s$ and $\hat{\tau}_{rzs} = \hat{\mu}(\partial \hat{u}_z / \partial r + \partial \hat{u}_r / \partial z)_s$. At low to moderate pressures, the viscosity of the vapor phase is much smaller than that of the corresponding liquid phase for a given fluid, i.e., $\mu \gg \hat{\mu}$. Thus, viscous stresses in the condensate film are much larger than in the vapor core. Therefore, Eqs. (3) and (4) may be approximated as

$$\tau_{rrs} \approx -\hat{p} + \sigma [1/r_s + (\partial^2 r_s / \partial z^2) / (1 + (\partial r_s / \partial z)^2)^{3/2} - 1/a] \quad (7)$$

$$\tau_{rzs} \approx 0. \quad (8)$$

Eq. (8) implies that for the disturbed flow in the vapor core, the viscous term may be neglected. Following the usual practice in the analysis of fluid flow in a cylindri-

cal tube, we assume that variations in pressure across the vapor core may be neglected, i.e., $|\partial\hat{p}/\partial r|\ll|\partial\hat{p}/\partial z|$. Furthermore, we assume that $U\gg\hat{u}_z$, \hat{u}_r ; thus, $\hat{u}_z^y\gg\hat{u}_r^y=\hat{u}_r$ and $\hat{\mathbf{u}}^y\cdot\nabla\hat{\mathbf{u}}^y\approx U\mathbf{n}_z\cdot\nabla\hat{\mathbf{u}}$. Based on the preceding, Eq. (5) may be reduced to

$$\frac{\partial\hat{u}_z}{\partial t} + U\frac{\partial\hat{u}_z}{\partial z} \approx -\frac{1}{\hat{\rho}}\frac{\partial\hat{p}}{\partial z}. \tag{9}$$

It follows that the induced flow in the vapor core can be modeled as a potential flow, $\hat{\mathbf{u}}=\nabla\phi$, where ϕ is a velocity potential. Note that in this case, $\nabla\cdot\hat{\mathbf{u}}^y=\nabla\cdot\hat{\mathbf{u}}=\nabla\cdot\nabla\phi=\nabla^2\phi=0$; i.e., Eq. (6) becomes the Laplace equation:

$$\frac{\partial^2\phi}{\partial r^2} + \frac{1}{r}\frac{\partial\phi}{\partial r} + \frac{\partial^2\phi}{\partial z^2} = 0. \tag{10}$$

Substituting $\hat{u}_z=\partial\phi/\partial z$ into Eq. (9) and integrating with respect to z yields

$$\frac{\partial\phi}{\partial t} + U\frac{\partial\phi}{\partial z} = -\frac{\hat{p}}{\hat{\rho}}. \tag{11}$$

2.2. Characteristic equation for condensate-film instability

If the vapor–liquid interface is initially perturbed infinitesimally and deformation of the interface is assumed to be sinuous; the radius of the disturbed interface can be described as [15,19,20]:

$$r_s = a + \alpha \cos kz \tag{12}$$

where a is the undisturbed radius of the inner surface of the condensate film $\alpha=\alpha_0 e^{\omega t}$ is the disturbance amplitude with α_0 being the amplitude of the initial disturbance, ω the growth rate in amplitude, and k the disturbance wavenumber.

To determine the volume integrals in Eq. (1), the condensate film is modeled as a one-dimensional Cosserat continuum [21]; thus,

$$\frac{\partial A}{\partial t} + \frac{\partial(Au_z)}{\partial z} = 0 \tag{13}$$

where $A=\pi(r_0^2-r_s^2)$ is the cross-sectional area of the condensate film. Eq. (13) yields the following expression:

$$u_r = \frac{\alpha_0\omega e^{\omega t} \cos kz}{am} r \left(\frac{r_0^2}{r^2} - 1 \right) \tag{14}$$

where $\eta\equiv ka$ and $m\equiv r_0^2/a^2-1$ ($m\neq 0$). Continuity for the condensate film yields

$$u_z = -\frac{2\alpha_0\omega e^{\omega t}}{\eta m} \sin kz. \tag{15}$$

Substituting the above expressions for u_r and u_z to the kinetic-energy and energy-dissipation terms in Eq. (1) gives:

$$\int_V \frac{\partial}{\partial t} \left(\frac{1}{2} \rho u_i u_i \right) dV = \frac{\pi^2 \alpha_0^2 \rho a^3 \omega^3 e^{2\omega t}}{2\eta^3 m} (8 + m\eta^2) \tag{16}$$

$$\int_V \tau_{ij} \epsilon_{ij} dV = \frac{\pi^2 \alpha_0^2 a \mu \omega^2 e^{2\omega t}}{2m\eta} (24 + 8R + m\eta^2) \tag{17}$$

where $n\equiv 1-3R^2+(4R^4 \ln R)/m$ and $R\equiv r_0/a$. The above integration was performed over a single wavelength, i.e., between $z=0$ and $2\pi/k$. The work term in Eq. (1) may be approximated as (note that only the terms normal to the interface are of interest)

$$\int_S \tau_{ij} u_i n_j dS \approx \int_S \tau_{rr} u_r n_r dS + \int_S \tau_{rz} u_z n_r dS. \tag{18}$$

Substituting Eqs. (7) and (8) into Eq. (18) and noting that the outward normal of the film is opposite that of the vapor core gives

$$\int_S \tau_{ij} u_i n_j dS \approx \int_S \hat{p} u_r dS - \int_S \sigma [1/r_s + (\partial^2 r_s / \partial z^2)] (1 + (\partial r_s / \partial z)^2)^{3/2} - 1/a u_r dS \tag{19}$$

where we have used the interfacial conditions given by Eqs. (2)–(4). With the aid of Eqs. (12) and (14), the second term on the right-hand-side of Eq. (19) becomes

$$\int_S \sigma [1/r_s + (\partial^2 r_s / \partial z^2)] (1 + (\partial r_s / \partial z)^2)^{3/2} - 1/a u_r dS = -2\pi^2 \alpha_0^2 \omega e^{2\omega t} \sigma (1 - \eta^2) / \eta. \tag{20}$$

Solving for ϕ from Eq. (10) subject to interfacial conditions given by Eqs. (2), (7) and (8), and substituting ϕ into Eq. (11) and rearranging, yields

$$\hat{p} = -\alpha_0 e^{\omega t} \frac{I_0(kr)}{I_1(\eta)} \left(\frac{\omega^2 \hat{\rho}}{k} \cos kz - 2\hat{\rho} U \omega \sin kz - \hat{\rho} U^2 k \cos kz \right) \tag{21}$$

where I_0 and I_1 are zeroth- and first-order modified Bessel functions of the first kind. Substituting Eqs. (21) and (15) into the first term on the right-hand-side of Eq. (19) gives

$$\int_S \hat{p}u_r \, dS = \frac{2\pi^2\alpha_0^2 e^{2\omega t} \hat{\rho}}{\eta^2} \frac{I_0(\eta)}{I_1(\eta)} (-a^3\omega^3 + a\omega U^2\eta^2). \quad (22)$$

Substituting Eqs. (16), (17), (20) and (22) into Eq. (1) yields the following dimensionless characteristic equation for the condensate-film instability:

$$\left[1 + \frac{4m\eta}{8 + m\eta^2} \frac{\hat{\rho}}{\rho} \frac{I_0(\eta)}{I_1(\eta)} \right] \beta^2 + 2Z\eta^2\beta = 8m\eta^2 \frac{1 - \eta^2}{8 + m\eta^2} + 4m\hat{W}_e \frac{\eta^3}{8 + m\eta^2} \frac{I_0(\eta)}{I_1(\eta)} \quad (23)$$

where $\beta \equiv \omega(2\rho a^3/\sigma)^{1/2}$ is the dimensionless growth rate in amplitude, $Z \equiv (3 + R^2)\mu/(2a\rho\sigma)^{1/2}$ is a modified Ohnesorge number (a dimensionless parameter representing the ratio of viscous to surface-tension forces) for the condensate, and $\hat{W}_e \equiv 2a\hat{\rho}U^2/\sigma$ is the Weber number (a dimensionless parameter describing the relative importance of hydrodynamic to surface-tension forces) based on the vapor phase. The condensate film is unstable whenever $\beta > 0$ ($\omega > 0$). In Eq. (24), the second term in the coefficient for β^2 indicates the influence of the vapor-liquid density ratio on the film instability; the coefficient for β denotes the effect of the viscosity on the film instability; the first and second terms on the right-hand-side represent the sources of instability, i.e. surface tension and the hydrodynamic forces, respectively. It is relevant to note that Eq. (23) is an explicit equation for the determination of β . If we have used the conventional approach [10], the characteristic equation would be implicit and in complex form which is much more difficult to solve.

3. Disturbance waves on the condensate film

According to Rayleigh's linear instability theory [22], from an initial disturbance a number of unstable waves may form at the vapor-liquid interface. The wave controlling the shape of the inner surface of the condensate film in a tube is the one having the maximum growth rate in amplitude, i.e., 'the most-unstable wave'. In this section, the most-unstable wave and the parameters that influence the most-unstable wave will be analyzed.

3.1. Case of low vapor velocities

The vapor velocity is changing along the tube during the condensation process, especially in heat-pipe condensers. In a small-diameter-thermosyphon, the vapor velocity is low in most parts of the condenser because in the dead-end zone of the condenser the vapor is almost stagnant. At low vapor velocities, $\hat{W}_e \rightarrow 0$; thus, Eq. (23) reduces to

$$\left[1 + \frac{4m\eta}{8 + m\eta^2} \frac{\hat{\rho}}{\rho} \frac{I_0(\eta)}{I_1(\eta)} \right] \beta^2 + 2Z\eta^2\beta = 8m\eta^2 \frac{1 - \eta^2}{8 + m\eta^2}. \quad (24)$$

In this case, $\beta > 0$ whenever $\eta < 1$ (i.e., $\lambda > 2\pi a$); thus, at low vapor velocities, instability of the condensate film is induced by long disturbance waves. For film thickness of the practical interest, $R \leq 2$; thus, $m, n < 4$. Noting that $\hat{\rho}/\rho \ll 1$, $I_0(\eta)/I_1(\eta) \approx 2/\eta$ and $m\eta^2 \ll 8$ for $\eta < 1$, Eq.(24) can be reduced to

$$\beta^2 + 2Z\eta^2\beta = m\eta^2(1 - \eta^2). \quad (25)$$

It is seen from Eq. (25) that the Ohnesorge number Z has a damping effect on the film instability because $\beta \rightarrow 0$ as $Z \rightarrow \infty$. The most-unstable wavenumber η_m may be determined by applying the condition $d\beta/d\eta|_{\eta_m} = 0$ to Eq. (25) to give:

$$\eta_m = \left[\frac{\sqrt{m}}{2(\sqrt{m} + Z)} \right]^{1/2}. \quad (26)$$

Eq. (26) implies that, in general, the condensate-film instability is dependent on film thickness (a) and viscosity of the condensate (μ).

Most of the working fluids used in phase-change heat exchangers are of low-viscosity. For such fluids (e.g., water and refrigerants), Z is of order of 10^{-2} or less if $R \leq 2$. Thus, in practice $\sqrt{m} \gg Z$. Therefore, for the condensate film in a tube, Eq. (26) becomes

$$\eta_m = 1/\sqrt{2} = 0.707. \quad (27)$$

Eq. (27) shows that for low vapor velocities, the most-unstable wavenumber is approximately constant, independent of film thickness and fluid properties of either phase. Instability of an annular viscous-liquid film in a small-diameter tube with a stagnant gas core was investigated experimentally as well as numerically by [10]. The measured disturbance wavenumbers fell in a range between 0.57 and 0.70 with $1.1 < R < 1.6$, having an average value $\eta = 0.65$ and no obvious film-thickness influence was evident. The prediction of this study is in good agreement with the measurement with the average difference between the prediction of this study and the experimental data being only 9%. The result of this study agrees excellently with Goren's numerical solutions of his implicit, complex characteristic Eq. [10]: the maximum difference in the range of R for which Goren investigated is less than 7%.

3.2. Case of high vapor velocities

Vapor velocities in the zone connecting with the adiabatic section in the condenser and in the evapor-

ator of a thermosyphon are higher than in the dead-end zone of the condenser. In these zones, both the maximum growth rate and the most-unstable wavenumber are functions of all of the parameters in Eq. (23). As was mentioned previously, values of the modified Ohnesorge number may be very small for the working fluids used in phase-change heat exchangers; thus, the damping effect (i.e. the second term) in Eq. (23) may be neglected. It follows that β can be solved from Eq. (23) as

$$\beta = (F_1 + F_2)^{1/2} / F_3^{1/2} \tag{28}$$

where

$$F_1 = 8m\eta^2 \frac{1 - \eta^2}{8 + m\eta^2}$$

$$F_2 = 4m\hat{W}_e \frac{\eta^3}{8 + m\eta^2} \frac{I_0(\eta)}{I_1(\eta)}$$

and

$$F_3 = 1 + \frac{4m\eta}{8 + m\eta^2} \frac{\hat{\rho}}{\rho} \frac{I_0(\eta)}{I_1(\eta)}$$

represent the influences of surface tension, the hydrodynamic force, and the vapor–liquid density ratio on the growth rate, respectively. Eq. (28) shows that β increases as F_2 ($F_2 \geq 0$) increases, and $\beta \rightarrow \infty$ as $F_2 \rightarrow \infty$, i.e., the hydrodynamic force has a destabilizing effect; β decreases as F_3 ($F_3 \geq 0$) increases and $\beta \rightarrow 0$ as $F_3 \rightarrow \infty$, i.e., the density ratio has a stabilizing effect. At high vapor velocities, the effect of surface tension on film instability is wavenumber dependent: if $\eta < 1$, then $F_1 > 0$, i.e., surface tension destabilizes the condensate film; if $\eta > 1$, then $F_1 < 0$, i.e., surface tension has a stabilizing influence.

A numerical analysis based on Eq. (28) indicates that both the maximum growth rate β_m and the most-unstable wavenumber η_m increase as \hat{W}_e increases. Thus, the disturbance waves in high vapor-velocity zones are shorter and grow faster than those in low vapor-velocity zones. The film thickness influences both β_m and η_m only limited at given values of $\hat{\rho}/\rho$ and \hat{W}_e . For example, at $\hat{\rho}/\rho = 0.001$ and $\hat{W}_e = 10$, the most-unstable wavenumber η_m varies between 3.6 and 3.8 over a range $R = 1.2$ – 1.5 . The dependence of the maximum growth rate β_m on film thickness at $\hat{\rho}/\rho = 0.001$ and $\hat{W}_e = 10$ is presented in Table 1. It is seen from this table that the maximum growth rate varies with film thickness only slightly. However, for a given Weber number, the $\beta_m = \beta_m(R)$ relationship results in a critical thickness at which the disturbance wave grows most rapidly (in Table 1, the critical thickness occurs at $R = 1.49$).

Table 1

Selected values for $\beta_m = \beta_m(R)$ at $\hat{\rho}/\rho = 0.001$ and $\hat{W}_e = 10$

R	1.30	1.40	1.48	1.49	1.50	1.60	1.70
β_m	7.628	7.968	8.045	8.047	8.046	7.986	7.855

In comparison with that at low vapor velocities, the vapor–liquid interface at high vapor velocities is often irregular because disturbance waves break up easily due to a large hydrodynamic interfacial force. However, in reality, breakup of the condensate film due to the hydrodynamic force occurs seldomly in small-diameter-tube condensers albeit it is encountered in the evaporators where the hydrodynamic force may be much larger than the capillary force. The mechanism for breakup of disturbance waves due to the hydrodynamic force is very complicated [23–25]. Detailed discussions may be found in [25]. To date, no experiments on the modes of most-unstable waves for high vapor velocities have been reported. Thus, comparison of this study with experiments is currently not available.

4. Discussion: interfacial phenomena in capillary condensation

As mentioned in the ‘Introduction’, liquid bridging caused by breakup of the condensate film may induce capillary blocking in small-diameter-thermosyphon condensers. Breakup of the condensate film, liquid bridging, and capillary blocking in small-diameter-thermosyphon condensers are all originated from the capillary instability. A condensation process that is associated with various capillary phenomena may be characterized as capillary condensation. In this section, we will discuss the interfacial phenomena in capillary condensation taking place in a small-diameter-thermosyphon condenser.

4.1. Breakup of the condensate film

In a thermosyphon, the condensate flows to the evaporator from the dead end of the condenser while the vapor flows to the dead end of the condenser from the evaporator. Because of the vapor condensation, the condensate film thickens during its downward flow. It has been discussed that deformation of the condensate film is governed by the most-unstable wave at the vapor–liquid interface. According to Eq. (13), the disturbed radius of the inner surface of the condensate film in a small-diameter-thermosyphon condenser may be expressed as

$$r_s = a + \alpha_0 e^{\omega_m t} \cos(2\pi z / \lambda_m) \tag{29}$$

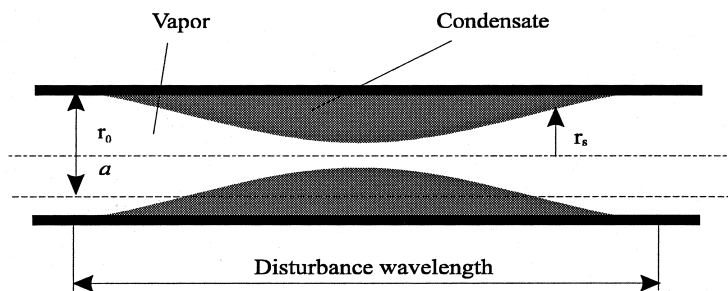


Fig. 3. A condensate collar in the condenser.

where ω_m is the dimensional maximum growth rate and $\lambda_m (\equiv 2\pi a / \eta_m)$ is the most-unstable wavelength. Since the vapor velocity and the thickness of the condensate film are different in different zones in the condenser, characteristics of disturbance waves may also be different. In the upper part of the condenser (i.e., the dead-end zone), the vapor is almost stagnant and the condensate film is thin; thus, the growth rate and wavelength of the disturbance wave can be determined from Eqs. (25) and (27) as $\omega_m = [(R^2 - 1)\sigma / (8\rho a^3)]^{1/2}$ and $\lambda_m = \sqrt{8\pi a}$. While in the lower part of the condenser (i.e., the zone near the adiabatic section), the vapor velocity is relatively high and the condensate film is thick. Therefore, ω_m and λ_m need to be solved from Eqs. (28) or (23). Based on the preceding analysis and Eq. (29), disturbance waves in the lower part of the condenser are shorter and grow faster than those in the upper part. (Considering that the Weber number is defined on the vapor phase, if the condensation pressure is low, then the hydrodynamic force in a small-diameter-tube condenser may not influence the most-unstable wavenumber significantly; thus, in the entire condenser, $\lambda_m \approx \sqrt{8\pi a}$.)

From the previous assumption, disturbance waves grow sinusoidally (an implication of this assumption is that the nonlinear effect due to finite initial disturbances on development of disturbance waves is neglected). Development of a disturbance wave then may be described by Eq. (29) with $r = a$ being the equilibrium position and $\cos(2\pi z / \lambda_m) = \pm 1$ denoting the trough and crest of the disturbance wave. Growth of a disturbance wave is restrained by two limits. One limit occurs when the wave trough reaches the tube wall. At this limit, the condensate film breaks up into a liquid collar (shown in Fig. 3). Under the sinusoidal-growth assumption, the thickness of the condensate film at the wave crest is, approximately, twice of the undisturbed condensate-film thickness. Thus, the disturbed radius at the wave crest is $r_{s,\text{crest}} = r_0 - 2(r_0 - a) = a(2 - R)$ and the corresponding wave-breakup time is $t_b = (1/\omega_m) \ln [(a/\alpha_0)(R - 1)]$. In this limiting case, $r_{s,\text{crest}} > 0$ (i.e., $R < 2$) and $r_{s,\text{trough}} \rightarrow r_0$. The other limit takes place at the condition $R \geq 2$. At this limit, the wave crest meets

the center line of the tube, i.e., $r_{s,\text{crest}} = 0$, $r_{s,\text{trough}} \leq r_0$ and the wave-breakup time is $t_b = (1/\omega_m) \ln(a/\alpha)$ (noting that the relationship $r_{s,\text{crest}} = a(2 - R)$ does not apply to the case $R > 2$). The surface energy of a liquid collar is larger than that of a liquid bridge of the same volume; thus, once the wave crest from both sides contacts at the center line of the tube, the liquid collar breaks up into a liquid bridge. The minimum thickness of the undisturbed film for this limiting case is $\delta = r_0/2$ (i.e., $R = 2$). However, if the nonlinear effect on the wave development is not negligible, then liquid bridging may also occur at the condition $R < 2$ [6].

Characteristics of disturbance waves suggest that breakup of the condensate film in a small-diameter-thermosiphon condenser may have different patterns in different zones in the condenser. In the upper part of the condenser where the thickness of the condensate film is less than $r_0/2$, the condensate film may break up into liquid collars, while in the lower part of the condenser where the thickness of the condensate film reaches $r_0/2$, liquid bridges may be produced from the film breakup.

4.2. Breakup of condensate collars

Formation of the first liquid bridge from the film instability in the lower part of the condenser blocks the vapor transport to the upper part of the condenser. It also induces a large capillary resistance to the condensate transport to the evaporator because the capillary force at the top vapor-liquid interface of the liquid bridge tends to prevent the condensate from flowing to the evaporator. Since its thickness is less than $r_0/2$, as discussed previously, the condensate film blocked may break up into liquid collars. Because of the vapor condensation, the tube wall between two liquid collars is always wetted with a thin film of the condensate. Since the condensate forming liquid collars is subcooled due to hysteresis in returning to the evaporator, the vapor blocked in the space above the liquid bridge will condense continuously which causes increase in volume of liquid collars. The volume of a liquid collar may be expressed as

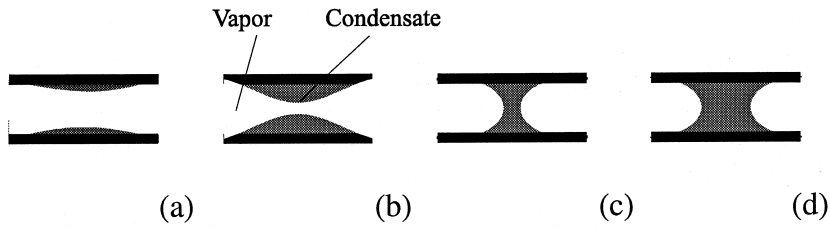


Fig. 4. Development of a condensate collar: time advances from (a)–(d).

$$V_{\text{collar}} = \pi \int_0^{\lambda_m} (r_0^2 - r_s^2) dz \quad (30)$$

where r_s is given by Eq. (29) and the disturbance wavelength may be approximated as $\lambda_m \approx \sqrt{8\pi}a$. Since λ_m is a fixed value for a given liquid collar, the shape of the liquid collar varies with changes in its volume.

The stability of a liquid collar is a function of the area-to-volume ratio $A_{\text{collar}}/V_{\text{collar}}$, where A_{collar} is the vapor–liquid interface area of the liquid collar. If the evolution of the liquid collar is assumed to be along a line of Laplace equilibria, then the following relationship holds: $C = \partial A_{\text{collar}}/\partial V_{\text{collar}}$, where C is the mean curvature of the liquid collar. When the volume of the liquid collar reaches a critical value $V_{\text{collar,cr}}$ at which $\partial C/\partial V_{\text{collar}} = 0$ (or $\partial^2 A_{\text{collar}}/\partial V_{\text{collar}}^2 = 0$), the liquid collar becomes unstable (the corresponding capillary instability is known as the Laplace instability) and breaks up into a liquid bridge [26]. Fig. 4 illustrates the development of a liquid collar with continuous vapor condensation. If we introduce a pseudo radius a_{cr} (in reality, $a_{\text{cr}} \approx a$) to describe the corresponding ‘undisturbed condensate film’, then mass conservation leads to $V_{\text{collar,cr}} = \pi(r_0^2 - a_{\text{cr}}^2)\lambda_m$. This relationship may be expressed alternatively as $V_{\text{collar,cr}}/\sqrt{8\pi^2 a_{\text{cr}}^3} \approx (R_{\text{cr}}^2 - 1)$, where $R_{\text{cr}} \equiv r_0/a_{\text{cr}}$. Based on the theoretical and experimental studies of [6], $R_{\text{cr}} = 1.1\text{--}1.2$. Because a film thickness with $R > 1.1$ can be reached easily, most of the liquid collars formed will break up into liquid bridges. However, because of variations in initial volumes (due to changes in film thickness with locations), different bridge widths are possible. This explains the non-equal-width liquid bridges reported by [9].

4.3. Mechanism for capillary blocking

Capillary blocking in thermosyphons of various tube diameters has been investigated by [8]. In their experiments, capillary blocking always occurred in thermosyphon condensers of 1- and 3-mm inside diameter (I.D.) while it took place in a 5-mm I.D. thermosyphon condenser only at high condensation heat-transfer rates, i.e., in cases where the condensate film was

thick. For condensers with inside diameters larger than 5 mm, no capillary blocking was observed. According to the observations of [8], the first liquid bridge formed commonly in the lower part of a small-diameter-thermosyphon condenser, and then the condensate and the vapor blocked above the liquid bridge formed a liquid plug which blocked the dead end of the condenser. Blocking of the dead end of the condenser with a liquid plug influences considerably the performance of the thermosyphon: the liquid plug at the dead end of the condenser reduces the effective length of the condenser which makes the condenser not work properly at the design condition, and, since the amount of the working fluid in circulation becomes much less than that in the design condition, partial dryout in the evaporator of the thermosyphon will be encountered, which, accordingly, reduces the heat-transport capacity of the thermosyphon significantly. In an extreme case, the evaporator may dry out completely [9].

Based on the preceding discussion and capillary phenomena reported by [8,9] [see Fig. 5(c) and (d)], we propose a plausible mechanism for capillary blocking in a small-diameter-thermosyphon condenser as follows. We assume that initially the two-phase-flow pattern in a small-diameter thermosyphon is of the usual type, i.e., an annular liquid film that covers the entire tube wall and a vapor core in the center of the tube [13,14]. Furthermore, we assume that as in normal working conditions of a heat pipe, only a small amount of liquid remains at the dead end of the evaporator, and that the condensate film is negligibly thin at the dead end of the condenser. Due to the interfacial instability, surface waves form at the vapor–liquid interface. As we discussed in the preceding, the unstable waves in the lower part of the condenser grow faster than those in the upper part; thus, we assume that the first liquid bridge forms in the lower part of the condenser, provided that the condensate film is thick enough to induce liquid bridging. Because growth rates of the disturbance waves also are dependent of the initial disturbance amplitudes which are distributed randomly on the condensate film, the first liquid bridge is not always necessary to form at the exit of the condenser where the maximum film thickness in the thermosyphon is reached. This first liquid

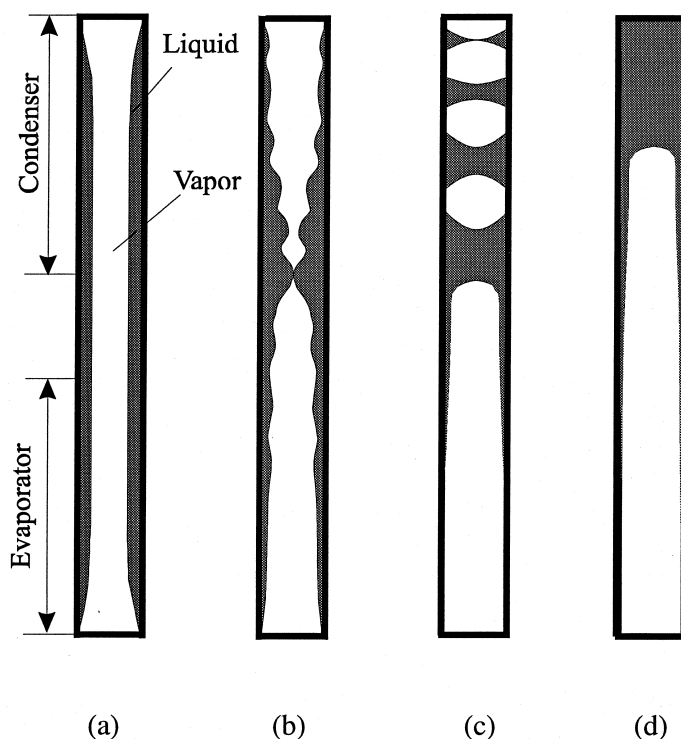


Fig. 5. Formation of liquid blocking: time advances from (a)–(d).

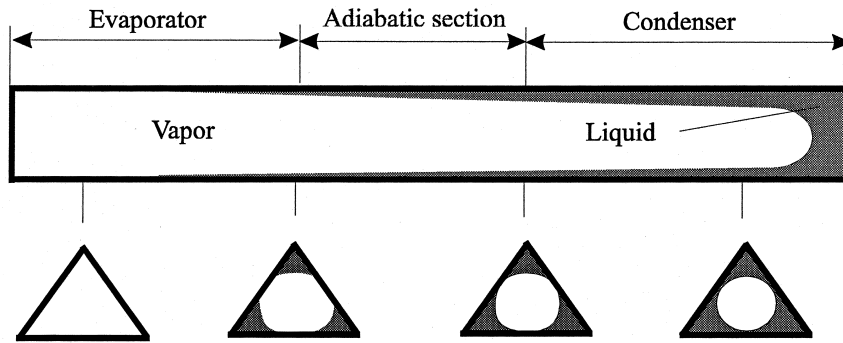
bridge blocks the vapor transport to the condenser and causes hysteresis in the transport of the condensate to the evaporator. Because thickness of the condensate film is relatively thin in the space blocked, breakup of the condensate film results in liquid collars. Most of these liquid collars are unstable and they further break up into liquid bridges of various bridge widths.

The liquid bridges cut the vapor blocked into bubbles. Due to buoyant motion of the bubbles and the vapor pressure at the bottom vapor–liquid interface of the liquid bridge that causes the blockage, the liquid bridges move to the dead end of the condenser, during which the bubbles are condensed and liquid bridges coalesce to form a liquid plug at the dead end of the condenser. This process is illustrated in Fig. 5. The two-phase-flow patterns shown in Fig. 5(c) and (d) agree with those reported by [9]. At some circumstances, the rate of condensation heat transfer is low, and therefore, the condensate film may not be thick enough to cause liquid bridging in the condenser. In this case, liquid bridging may occur in the upper part of the evaporator due largely to a dynamic bridging mechanism [3–5]. Since the vapor velocity in the evaporator is high while in the blocked space the vapor is almost stagnant, the pressure difference over the liquid bridge formed is $\Delta p = \rho g l_{\text{bridge}} + 2\sigma(1/r_B - 1/r_T) > 0$, where r_B and r_T are the mean radii of the bottom and

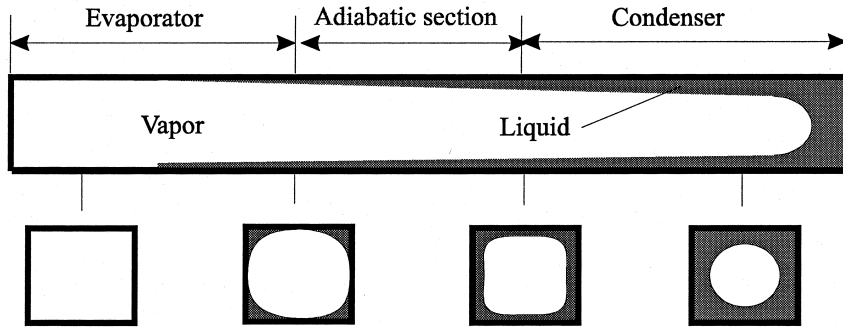
top vapor–liquid interfaces, and l_{bridge} is the width of the liquid bridge. Under this driving force, the liquid bridge may be pushed into the condenser. This ‘liquid pumping’ phenomenon may take place periodically until the liquid film becomes too thin and no liquid bridges can be formed. In this case most of the liquid bridges in the condenser may be ‘pumped’ there from the evaporator. Capillary blocking due to this liquid-pumping mechanism was observed by [9].

Although capillary blocking is originated from various capillary instabilities, the force that holds up the liquid plug at the dead end of the thermosyphon condenser is the pressure of the vapor below the liquid plug because both the gravitational and capillary forces tend to drive the condensate to flow to the evaporator (note that the pressure in the evaporator is higher than in the condenser in all kinds of heat pipes). Since the liquid plug is on the top of the vapor, the vapor–liquid interface forms a typical case of Taylor instability. However, if the tube diameter is small enough, the gravitational force becomes negligible in comparison to the capillary force, then the vapor–liquid interface may be considered to be stable. This explains why stable capillary blocking occurs only in small-diameter-thermosyphon condensers.

Capillary blocking also occurs in wickless micro head pipes [13,14]. Hydrodynamic and capillary



(a) Trigonal cross section.



(b) Tetragonal cross section.

Fig. 6. Capillary blocking and partial dryout in two different wickless micro heat pipes.

instabilities in wickless micro heat pipes with a polygonal cross section are very complicated and beyond the scope of this study. Here we only discuss some common phenomena in both small-diameter thermosyphons and wickless micro heat pipes. Fig. 6 shows capillary blocking and partial dryout phenomena in wickless micro heat pipes with trigonal and tetragonal cross sections. Because of the Gregorig effect, capillary forces in the corners are much larger than those at the planar surfaces, and thus, the partial-dryout phenomenon in a wickless micro heat pipe with a polygonal cross section is different from that in a small-diameter thermosyphon: in the former, partial dryout may be found in the entire evaporator due to the Gregorig effect, the liquid is not uniformly distributed and most of the planar surfaces could possibly be dry; in the latter, complete dryout occurs in the dead-end zone of the evaporator and beyond this zone the tube wall is wetted completely, i.e., part of the evaporator works in a normal way.

It should be pointed out that although capillary

blocking usually occurs in the condenser of a wickless micro heat pipe, it has a small effect on the overall condensational heat transfer because only a small portion of the condenser is blocked with the condensate; in comparison, it impacts the overall evaporation heat transfer significantly because a large percentage of the surface area of the evaporator becomes dry, i.e., two-phase heat transfer occurs only in part of the surface of the evaporator. Therefore, capillary blocking has a significant impact on the heat-transport capacity of wickless micro heat pipes and small-diameter thermosyphons. The dry surface in the evaporator of either a small-diameter thermosyphon or a wickless micro heat pipe may be reduced by increasing the filling ratio. However, a large filling ratio will not prevent capillary blocking, and it will reduce the evaporation area of the evaporator, which, accordingly, will also influence the heat-transport capacity. In applications of either small-diameter thermosyphons or wickless micro heat pipes, their characteristics must be taken into consideration. For example, how the surfaces of evaporators in con-

tact of the heat source is an important factor because at the unwetted surfaces of the evaporators heat transfer is of a single-phase type.

5. Summary and conclusions

A characteristic equation describing instability of the condensate film in a small-diameter-tube condenser was developed via an integro-differential approach. Instability of the condensate film was analyzed using the resultant equation. It is found that (1) in the zones of low relative vapor velocities, the cause of the film instability is the surface tension and wavelengths of the disturbance waves are approximately a function of the radius of the undisturbed inner condensate film, i.e., $\lambda_m \approx \sqrt{8\pi a}$; and (2) in the zones of high relative vapor velocities, the film instability is induced by the hydrodynamic force (due to the difference in phase velocities), and the larger the hydrodynamic force, the shorter the disturbance wave and the faster they grow. These predicted characteristics of the disturbance waves agree with experimental observations and measurements reported in the literature.

On the basis of the resultant characteristic equation, the mechanism for capillary blocking that occurs in a small-diameter-thermosyphon condenser was examined. Both Rayleigh instability which causes breakup of the condensate film and Laplace instability which induces break up of condensate collars into liquid bridges are found to be responsible for the capillary phenomena in the condenser. Due to these capillary instabilities, the condensate film in the condenser breaks up (directly as well as indirectly) into liquid bridges which block the vapor flow. Then, because condensation of the vapor between liquid bridges induces coalescence of the liquid bridges, and because the pressure in the evaporator is always higher than that in the condenser of a thermosyphon, the coalesced liquid bridges form a liquid plug and this liquid plug is pushed to the dead end of the condenser, resulting in capillary blocking. This proposed mechanism explains the experimental observations reported in the literature.

Since capillary instabilities that are encountered in small-diameter-thermosyphon condensers may occur in other small-channel condensations, and since the pressure distributions are similar in all kinds of heat pipes, capillary blocking may also take place in wickless micro heat pipes. Due to capillary blocking, the working fluid circulating in a wickless micro heat pipe becomes much smaller than that at the design condition, which may result in partial dryout in the evaporator. Because the majority of the wickless micro heat pipes have a polygonal cross section, in evaporators of these micro heat pipes liquid may be accumulated on

the corners and a large percentage of the planar surfaces may be dry. The partial-dryout characteristics of the evaporator must be considered in applications of the wickless micro heat pipes because no phase change occurs at the unwetted surfaces of the evaporators.

Acknowledgements

The authors would like to acknowledge the support of this work through a Hong Kong Research Council Grant (No. HKUST815/96E) and a KHUST Grant (No. TOO96/97-EG03).

References

- [1] V.P. Carey, *Liquid–Vapor Phase-Change Phenomena*, Hemisphere, Washington, 1992.
- [2] Lord Rayleigh, On the instability of cylindrical fluid surfaces, *Philosophica Magazine* 34 (1892) 177–180.
- [3] G.J. Zabararas, A.E. Dukler, Countercurrent gas–liquid annular flow, including the flooding state, *AIChE Journal* 34 (1988) 389–396.
- [4] R.K. Das, S. Pattanayak, Electrical impedance method for flow region identification in vertical upward gas–liquid two-phase flow, *Measurement Science and Technology* 4 (1993) 1457–1463.
- [5] R.K. Das, S. Pattanayak, Determination and analysis from annular to intermittent flow in vertical tubes, *Canadian Journal of Chemical Engineering* 74 (1996) 49–57.
- [6] P.A. Gauglitz, C.J. Radke, An extended evolution equation for liquid film breakup in cylindrical capillaries, *Chemical Engineering Science* 43 (1988) 1457–1465.
- [7] S. Middleman, *Modeling Axisymmetric Flows: Dynamics of Films, Jets, and Drops*, Academic Press, New York, 1995.
- [8] L.L. Vasil'ev, S.V. Konev, R. Razeq, Investigation of capillary blocking of heat-pipe condensers, *Heat Transfer—Soviet Research* 20 (1988) 692–701.
- [9] H.Z. Chen, M. Groll, S. Rösler, Micro heat pipes: experimental investigation and theoretical modeling, in: *Proceedings of the 8th International Heat Pipe Conference*, Beijing, 1992, pp. 396–400.
- [10] S.L. Goren, The instability of an annular thread of fluid, *Journal of Fluid Mechanics* 12 (1962) 309–319.
- [11] H.L. Goldsmith, S.G. Mason, The flow of suspensions through tubes II. Single large bubbles, *Journal of Colloid Science* 18 (1963) 237–261.
- [12] M. Ishii, Wave phenomena and two-phase flow instabilities, in: G. Hetsroni (Ed.), *Handbook of Multiphase Systems*, McGraw-Hill, New York, 1982 Section 24.
- [13] G.P. Peterson, *An Introduction to Heat Pipes: Modeling, Testing, and Applications*, John Wiley and Sons, New York, 1994.
- [14] A. Faghri, *Heat Pipe Science and Technology*, Taylor and Francis, Washington, 1995.

- [15] Lord Rayleigh, On the instability of jets, London Mathematical Society Proceedings 10 (1878) 4–18.
- [16] R. Aris, Vectors, Tensors, and the Basic Equations of Fluid Mechanics, Dover, New York, 1989.
- [17] C.M. Kinoshita, H. Teng, S.M. Masutani, A study of the instability of liquid jets and comparison with Tomotika's analysis, International Journal of Multiphase Flow 20 (1994) 523–533.
- [18] L.D. Landau, E.M. Lifshitz, Fluid Mechanics, Pergamon Press, New York, 1993.
- [19] C. Weber, On the breakup of a liquid jet, Zeitschrift für Angewandte Mathematic und Physik 11 (1931) 136–154.
- [20] S. Tomotika, Breakup of a drop of viscous liquid immersed in another viscous fluid which is extending at a uniform rate, Proceedings of the Royal Society of London A153 (1936) 302–318.
- [21] D.B. Bogoy, Use of one-dimensional Cosserat theory to study instability in a viscous liquid jet, Physics of Fluids 21 (1978) 190–197.
- [22] Lord Rayleigh, Theory of Sound, Dover, New York, 1945.
- [23] G.B. Wallis, The Onset of Droplet Entrainment in Annular Gas–Liquid Flow. General Electric Report, No. 62 GL127, 1962.
- [24] S. Levy, Prediction of two-phase annular flow with liquid entrainment, International Journal of Heat and Mass Transfer 9 (1966) 171–188.
- [25] G.F. Hewitt, N.S. Hall-Taylor, Annular Two-Phase Flow, Pergamon Press, New York, 1970.
- [26] D.H. Everett, J.M. Haynes, Model studies of capillary condensation: I. Cylindrical pore model with zero contact angle, Journal of Colloid and Interface Science 38 (1972) 125–137.